applied sciences

MDPI

Article

Analytical Point-Cloud Based Geometric Modeling for Additive Manufacturing and Its Application to Cultural Heritage Preservation

Tashi [1], AMM Sharif Ullah [2,*], Michiko Watanabe [2] and Akihiko Kubo [2]

[1] Graduate School of Engineering, Kitami Institute of Technology, 165 Koen-cho, Kitami 090-8507, Japan; d1871308030@std.kitami-it.ac.jp

[2] Faculty of Engineering, Kitami Institute of Technology, 165 Koen-cho, Kitami 090-8507, Japan; michy@mail.kitami-it.ac.jp (M.W.); kuboak@mail.kitami-it.ac.jp (A.K.)

* Correspondence: ullah@mail.kitami-it.ac.jp; Tel./Fax: +81-157-26-9207

Received: 28 March 2018; Accepted: 22 April 2018; Published: 24 April 2018

Featured Application: Featured Application: Without relying on scanner or image processing, one can use the presented work to create rapid prototypes of artifacts having cultural significance and beyond.

Abstract: Point-cloud is a valuable piece of information for geometric modeling and additive manufacturing of different types of objects. In most cases, a point-cloud is obtained by using the 3D scanners or by using image processing. Alternatively, one can rely on an analytical approach for creating the required point-cloud. In this study, we develop an analytical method that uses both equation and algorithm-based approaches for creating a point-cloud for modeling a given object (or shape). The analytically created point-cloud can then be processed by using a commercially available CAD package to create a virtual model (or solid CAD model) of the object. Finally, the virtual model can be used to create a physical model (or replica) of the underlying object using a commercially available additive manufacturing device (e.g., a 3D printer). The abovementioned procedure of analytical point-cloud based geometric modeling for additive manufacturing can be applied to preserve artifacts having cultural significance. In particular, we consider the Ainu motifs that represent the cultural heritage of Ainus living in the northern part of Japan (Hokkaido). We first classify the motifs and then model them in the form of a point-clouds using both equations and a recursive process (algorithm) proposed in this study. Finally, we create the CAD model and physical models of the artifacts having Ainu motifs on them. This way, we show the effectiveness of the analytical point-cloud based geometric modeling for additive manufacturing.

Keywords: point-cloud; additive manufacturing; geometric modeling; cultural heritage; Hokkaido Ainu

1. Introduction

In contrary to the conventional manufacturing processes (e.g., subtractive manufacturing processes, such as, milling, drilling, turning, and alike), Additive Manufacturing (AM) processes have been introduced to manufacture physical objects by adding materials layer by layer [1]. AM (also known as 3D printing (3DP), rapid prototyping, or freeform fabrication) can now be used to manufacture objects having complex shapes and multi-scale structures. AM can also manufacture objects by adding different types of materials at different layers. As a result, AM has transformed the way that the objects are being designed and manufactured [2–4]. AM is now applied to manufacture automotive parts [5], aerospace parts [2], biomedical products (e.g., dental braces, artificial tissues,

hearing aids, dummy cadaver, and prosthetic) [6–12], educational objects [13–15], fashion items (e.g., cloth, shoes, and jewelry) [16–20], foodstuffs (e.g., pizza, chocolate, crackers, and pasta) [21–23], construction objects (e.g., 3D printed house) [24–26], and items for preserving and restoring cultural heritage [27]. Small, affordable, and user-friendly AM machines (e.g., 3D printers) are now available for running small businesses, too [28–30].

As schematically illustrated in Figure 1, a typical AM operation consists of the following five steps: (1) creation of a 3D computer-aided design (CAD) model of the desired object (virtual model); (2) triangulation of the CAD model (known as STL data); (3) slicing of triangulated CAD model; (4) execution of AM process; and (5) surface finishing of the physical model [1,2].

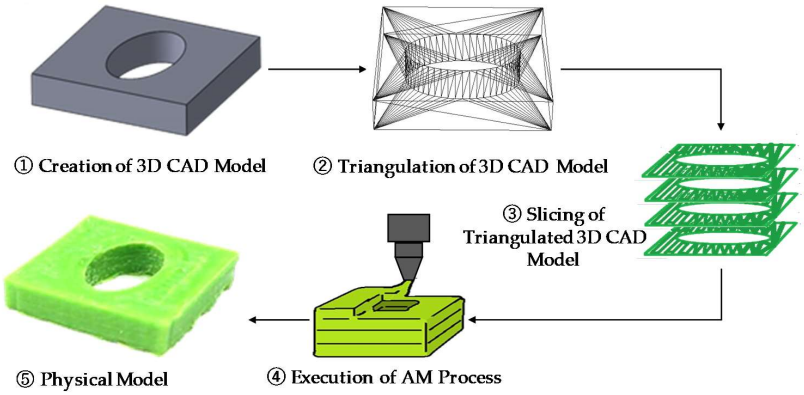

Figure 1. The working principle of Additive Manufacturing (AM).

However, the advent of AM has introduced a technology called Reverse Engineering (RE), as schematically illustrated in Figure 2. In RE based AM, a 3D scanner first scans an object and represents it by a relatively large number of points called point-cloud. Using a CAD package, the point-cloud is transformed into a solid CAD model. The CAD model can be modified as preferred by the user before manufacturing it by AM. Thus, RE is mainly used for preserving artistic and culturally significant objects by creating the replicas or manufacturing another object based on the physic of the existing object for which the solid CAD model is not available. See [10,11,31–35] for more details regarding RE.

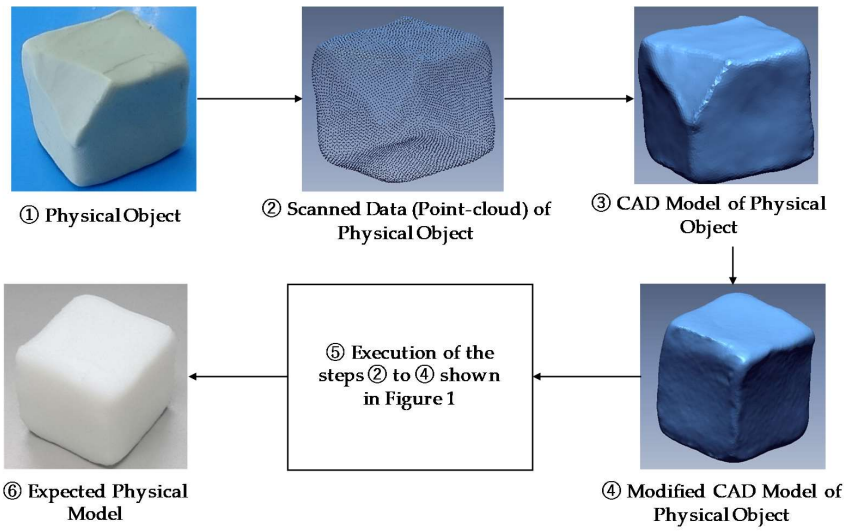

Figure 2. A workflow for Reverse Engineering (RE) based AM.

Nevertheless, as described in Figure 2, when a solid CAD model is not available in the first place, one can rely on the most primitive representation of an object, i.e., a point-cloud, and execute the steps shown in Figure 1. Therefore, point-cloud based geometric modeling has earned a great deal of attention from the AM community. However, it has been emphasized that the conventional CAD systems need additional functionalities to generate solid models of complex shapes (e.g., multi-scale cellular and lattice structures) from point-clouds [2]. In addition, creating a complex shape from a point-cloud using conventional CAD systems requires a great deal of skill, making it a heavily user-skill-dependent activity. This means that the typical steps of AM as shown in Figures 1 and 2 can be modified to accommodate the point-cloud in a befitting manner. This creates a notion called Point-Cloud based AM (PCAM). In most cases, a point-cloud is obtained by using the 3D scanners and processed before creating a CAD modeling. This issue is described elaborately in the literature review section. However, one can rely on some analytical approaches for creating the required point-cloud for PCAM. This direction of PCAM has not yet been explored compared to other direction, i.e., 3D-scanner based point-cloud creation for PCAM. Thus, the objective of this article is to shed some lights on an analytical point-cloud based AM. As an application, the cultural heritage preservation is considered.

Based on the abovementioned contemplation, this article is written. The remainder of this article is organized, as follows: Section 2 describes the relevant research work available in the literature regarding PCAM. Section 3 describes the proposed PCAM method that uses both equations and algorithmic approaches for creating a point-cloud for modeling a given object (or shape), as well as its CAD model and AM based prototype. Section 4 describes the application of the proposed PCAM in creating artifacts having cultural significance. In particular, the Ainu motifs that represent the cultural heritage of Ainus living in the northern part of Japan (Hokkaido) is considered. Section 5 provides the concluding remarks of this study.

2. Literature Review

This section described a relatively comprehensive literature review on the PCAM and closely related issues. In the literature, it has been found that both the data acquisition processes and the surface model creation techniques for PCAM have been covered in different angles. These two aspects of PCAM is reviewed in the following two sub-sections.

2.1. Data Acquisition Process for PCAM

Data acquisition has three aspects, namely, registration, noise removal, and data reduction that make a point-cloud meaningful to the CAD systems [36]. The registration process combines all the fragmented point-clouds into a coordinate system. The noise removal process removes the unwanted noises from the point-cloud. The data reduction process removes the redundant points from the point-cloud. It is worth mentioning that registration and noise removal processes are sometimes inseparable. These two aspects are described as follows.

Point-cloud registration methods are classified broadly into three categories: greedy searching-based, global feature-based, and local feature-based methods. See [37] for the details. To ensure an accurate and efficient point-cloud registration and noise removal, numerous researchers have developed different techniques or algorithms. Some of the selected research are briefly discussed as follows. Li and Song [38] have developed a modified iterative closest point algorithm based on dynamic adjustment factor for the registration of point-clouds and CAD modeling. The registration time is reduced significantly and registration accuracy is improved considerably, but the method's convergence process is very slow and needs many iterations. Zhao and Illius [39] have implemented machine learning algorithms combined with the shape descriptor to classify the 3D point-clouds. James et al. [31] have developed a photogrammetry color segmentation based technique as an alternative approach to scan and construct 3D point-cloud for RE applications. Watanabe et al. [40] have shown various ways for aligning the short-range point-clouds (captured by using a portable laser scanner) to a large-scale point-cloud (captured by using a terrestrial laser scanner). They aligned the point-clouds

in a reasonable time with good precision. Yap et al. [6] have implemented different types of data acquisition methods, such as engineering drawing, computed tomography, and optical coherence tomography, to build the 3D printed bio-models for medical applications. They observed that the data acquisition and conversion technique had a significant effect on the quality of the model. Syed et al. [41] have investigated the influence of the surface characteristics on the point-cloud. They acquired the point-cloud by using a laser scanning probe and observed that the surface characteristics affect the quality of the point-cloud, no matter the scanning accuracy. On the other hand, regarding the data reduction process, Lee and Woo [42] have developed an algorithm to remove the redundant points from a point-cloud to reduce the execution time for integration of RE and RP. Removing the redundant points from the point-cloud saves the computation time to a large extent.

2.2. Surface Model Creation Techniques for PCAM

Once the point-cloud is available and processed based on the aspects described above, a surface model creation is considered. Since the point-clouds are obtained from RE, a great emphasis is given on the creation of freeform surfaces. In this regard, the curve-based modeling and the polygon-based modeling are the most commonly used methods [36]. These issues are described as follows.

In the curve-based modeling, it includes three steps, namely, segmentation, curve fitting, and skinning. A Non-Uniform Rational B-Spline (NURBS) curves using the least square method is used in the curve-based modeling technique. For example, Fayolle et al. [43] have developed a construction tree model for surface model creation from the point-cloud. Schwartz et al. [44] have generated a 3D model by building a loft feature through some curves generated by slicing the point-cloud wherein the point-cloud data are obtained from 3D sketching. Xu et al. [45] have implemented a virtual approach for slicing the point-cloud for AM process. Haiqiao et al. [46] have developed the algorithms for generating blocked patterns automatically from the point-cloud data that can be used in garment manufacturing. Peternell and Steiner [47] have developed an algorithm for the surface reconstruction of a piecewise planar object or CAD model from the point-cloud. Pal [48] have developed a tangent plane method for generating 3D geometry from the point-cloud. Oropallo et al. [49,50] have implemented a point-cloud based approach to directly slicing of NURBS based model for 3DP rather than STL-based slicing. They used original NURBS model and converted the model into a point-cloud, and the applied direct slicing.

The polygon-based modeling (on the other hand) consists of four steps, namely, triangulation, decimation, subdivision, and triangle to NURBS fitting. The triangulation can be performed by using the methods called Delaunay triangulation, alpha shaping, crusting, and volumetric triangulation. Recently, many authors have improved the efficiency of the abovementioned methods. For example, Masuda et al. [32] have developed a method for a reconstruction of polygonal faces from the point-cloud and mapped each point-cloud onto a 2D image for detecting the bounded planar faces. Ma et al. [51] have developed an umbrella facet matching algorithm to construct the watertight manifold triangle meshes from the point-cloud. Zhong et al. [52] have developed an inverse distance square method for direct slicing of the spatial point-cloud data obtained from the RE for rapid prototyping [26] applications. They also implemented the extended extrapolation method to obtain a vertical slicing contour, wherein the contour points in each layer are searched, sorted, and reconstructed by interpolation of NURBS. Yang et al. [53] have developed an algorithm based on the moving least-squared process that can intersect with lines, planes, polygonal mesh, and NURBS surface for the direct manufacturing of object given by a massive point-cloud without building the CAD model. Percoco and Galantucci [54] have developed a genetic algorithm for direct slicing of the point-cloud for RP. It can be used to overcome the limitations of polygonization of the point-cloud. Chang et al. [55] have developed a method for surface reconstruction from the point-clouds for creating the textures on the surface which can be used in a medical scaffold.

It is worth mentioning that, compared to the curve-based modeling processes, the polygon-based modeling systems take less time regardless of the geometric complexity of the scanned parts. However,

it is still challenging to reconstruct the fine details, such as the sharp corners and edges using the methods mentioned above.

Apart from the point-clouds obtained by using data acquisition system, e.g., a 3D scanner, laser probe, and alike, as explained in above, a point-cloud can also be created by using mathematical process. Some authors have also worked in the other direction. For example, Ullah et al. [56–58] and Ullah [59] have created some point-clouds the using the mathematical processes called iterative function systems and Monte Carlo simulation. They have used the point-clouds as the base models and manufactured the self-similar objects (e.g., fractals) and porous structures. The issues related to the design for AM using mathematically generated point-cloud have also been discussed in [56].

3. Method

As described in the previous sections, the main emphasis of point-cloud based AM is on the point-clouds obtained by scanning the existing objects. Alternatively, one can create point-clouds using an analytical approach, which has not yet been studied elaborately, as mentioned in the previous section, too. Thus, this section describes the proposed method for PCAM as shown in Figure 3. In this approach, other than the analytical approach for creating the point-clouds, the CAD modeling and triangulation modeling are involved. As shown in Figure 3, first the point-cloud is created by the analytical approach. Then the point-clouds are transformed into solid models using CAD packages, which is referred to as CAD modeling. In the next step, the solid CAD models are used to create the triangulation model of the solids, which is referred to as triangulation modeling and the outcome (STL data) can be used in the AM for building physical models.

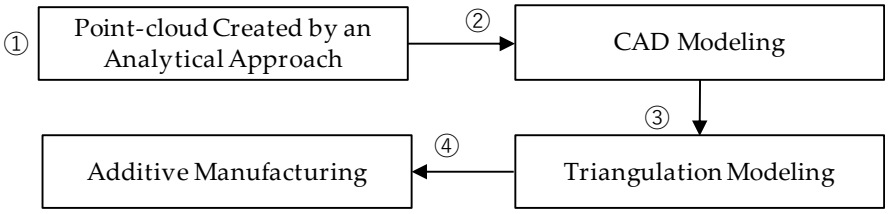

Figure 3. Proposed method for Point-Cloud based Additive Manufacturing (PCAM).

Now the question is how to create the point-clouds using the analytical approach? In this regard, there are two main approaches, namely, the deterministic point-cloud creation process and stochastic point-cloud creation process [59]. In deterministic point-cloud creation process, one can use two different procedures. One of the procedures uses a parametric-equation-based approach and the other uses an algorithmic approach. On the other hand, in stochastic point-cloud creation process, one can use a pure stochastic approach (e.g., a point-cloud that is created by Monte Carlo simulation of a variable that follows normal distribution [59]) or a semi-stochastic approach where some affine maps are used in a semi-stochastic manner (e.g., IFS fractals [56]). However, in this study, the deterministic approach is considered.

3.1. Parametric-Equation-Based Approach

In parametric-equation-based approach, a shape is modeled by a set of parametric equations. For example, consider the point-clouds shown in Figure 4. As seen in Figure 4, four shapes, namely, Line, Ellipse, Hexagon, and Bicorn curve are represented by four different point-clouds. These point-clouds are created by using the parametric-equation-based approach described in Appendix A. It is worth mentioning that the parametric curves (e.g., Bezier curves, B-Splines, and NURBS) also belong to this category. The number of points in the point-cloud depends on the discretization of the parameter involved, as described in Appendix A. The application of the point-clouds created by using parametric-equation-based approach is described in details in Section 4. However, for the sake of

better understanding, an example showing how to integrate these point-clouds with regard to Figure 3 is shown in Figure 5.

As seen in Figure 5a, first, some piece-wise straight-lines are considered; these lines are modeled by using a point-cloud created by the parametric equations defined in Equation (A1). Then the point-cloud is rotated by using Equations (A2) and (A3) to create the required teeth of the gear. The point-clouds of the teeth are transferred to CAD packages for CAD modeling. The result of CAD modeling is shown in Figure 5b. Nowadays, CAD packages can perform triangulation modeling, too. The result of triangulation modeling is shown in Figure 5c. The STL data generated from the triangulation modeling can then be used to manufacture a physical model of the gear using AM (e.g., 3D printing), as shown in Figure 5d.

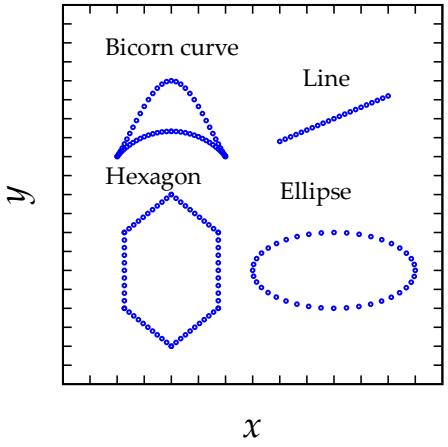

Figure 4. Point-clouds created by using the parametric-equation-based approach.

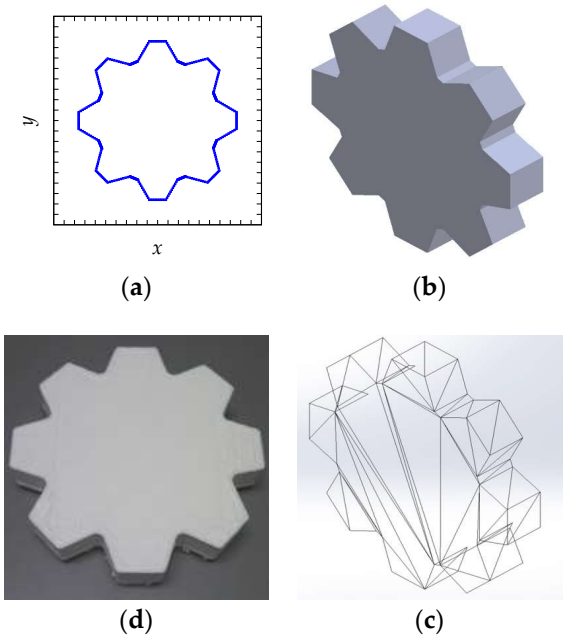

Figure 5. PCAM of gear model using parametric-equation-based approach. (**a**) Point-cloud of a gear created by the parametric equations of some piecewise lines; (**b**) CAD modeling of the gear; (**c**) Triangulation modeling of the gear; (**d**) Additive manufacturing (3D printing).

3.2. Algorithmic Approach

Sometimes it is not an essay task to image the right set of equations for creating a point-cloud using the method described in the previous sub-section. In this case, a point-cloud can be created recursively using an algorithmic approach. Ullah et al. [58] have shown an algorithmic approach where set points are created recursively by two user-defined parameters called distance and angle. We have modified their algorithm to the create point-cloud for geometric modeling. Steps to create a point-cloud based on a recursive process are as Algorithm 1:

Algorithm 1 Point-cloud Creation Algorithm

1. Define: Center Point $P_c = (P_{cx}, P_{cy}) \in \Re^2$, Length $d > 0$, Initial Angle $\alpha \in \Re$
2. Define: Instantaneous Distances $(r_i \in \Re \mid i = 1, ..., n)$
3. Define: Rotational Angles $(\rho_i \in \Re \mid i = 1, ..., n)$
4. Calculate: $P_0 = (P_{0x}, P_{0y})$ so that $P_{0x} = P_{cx} + d\cos\alpha$ and $P_{0y} = P_{cy} + d\sin\alpha$
   Iterate: For $i = 1, ..., n$
5. Rotate P_0 by an angle ρ_i around P_c in the counter-clockwise direction to create $P_i = (P_{ix}, P_{iy})$ so that
   $P_{ix} = P_{cx} + (P_{0x} - P_{cx})\cos\rho_i - (P_{0y} - P_{cy})\sin\rho_i$ and
   $P_{iy} = P_{cy} + (P_{0x} - P_{cx})\sin\rho_i + (P_{0y} - P_{cy})\cos\rho_i$
   Extend P_i to P_{ei} that is point on the line P_cP_i at a distance r_i from P_c
   $P_{eix} = P_{cx} + (P_{ix} - P_{cx})\frac{r_i}{d}$ and $P_{eiy} = P_{cy} + \left(P_{iy} - P_{cy}\right)\frac{r_i}{d}$
   End For
6. Output: Point-Cloud, PC = $\{P_{ei} \mid i = 1, ..., n\}$

The description of the algorithm is as followed. The algorithm consists of four steps: Step 1 is the input step. Step 2 is the calculation step. Step 3 is the iteration step. Step 4 is the output step. In the input step, the following entities are defined: Center Point $P_c = (P_{cx}, P_{cy}) \in \Re^2$, Length $d > 0$, Initial Angle $\alpha \in \Re$, Instantaneous Distances $(r_i \in \Re \mid i = 1, ..., n)$, and Rotational Angles $(\rho_i \in \Re \mid i = 1, ..., n)$. In the calculation step, $P_0 = (P_{0x}, P_{0y})$ is calculated, which is a point at a distance d and the line P_cP_0 makes an angle α in the counter-clockwise direction from the x-axis. In the iteration step, the points denoted as $P_i = (P_{ix}, P_{iy})$ are created by rotating P_0 at an angle ρ_i in the counter-clockwise direction from the x-axis. Afterward, the points $P_i = (P_{ix}, P_{iy})$ are placed at a distance r_i from P_c resulting $P_{ei} = (P_{ix}, P_{iy})$, $i = 1, ..., n$. In the output step, the points $P_{ei} = (P_{ix}, P_{iy})$, $i = 1, ..., n$, are collected for creating the desired Point-Cloud, i.e., PC = $\{P_{ei} \mid i = 1, ..., n\}$. Figure 6 schematically illustrates the algorithm up to two iterations. As seen from Figure 6, the algorithm creates points with respect to P_c and P_0 depending on the values of r_i and ρ_i. It can be used to create different kinds of planner shape. In this respect, the user needs to choose the right pairs of Instantaneous Distances $(r_i \in \Re \mid i = 1, ..., n)$ and Rotational Angles $(\rho_i \in \Re \mid i = 1, ..., n)$. To get more insights into the algorithm, three example shapes are created as shown in Figure 7. In particular, the point-clouds shown in Figure 7 correspond to a circle, a curvy shape, and a leaf.

As seen in Figure 7a for $\alpha = 5^\circ$, $r_i = 20$, $i = 1, ..., 37$, $\rho_1 = 0$, $\rho_2 = 10$, ..., $\rho_{37} = 360$ degrees, the points of the point-clouds correspond to the points on the circumference of a circle having a radius of 20 and the center at (5, 10). By linearly decreasing r_i and simultaneously increasing ρ_i and vice versa creates the point-cloud of a curvy shape as shown in Figure 7b. Systematic increase and decrease in both r_i and ρ_i or keeping ρ_i constant for certain instants creates the point-cloud of a leaf is shown in Figure 7c. The use of the algorithmic approach, along with the parametric-equation-based approach, will be presented in detail in the next section.

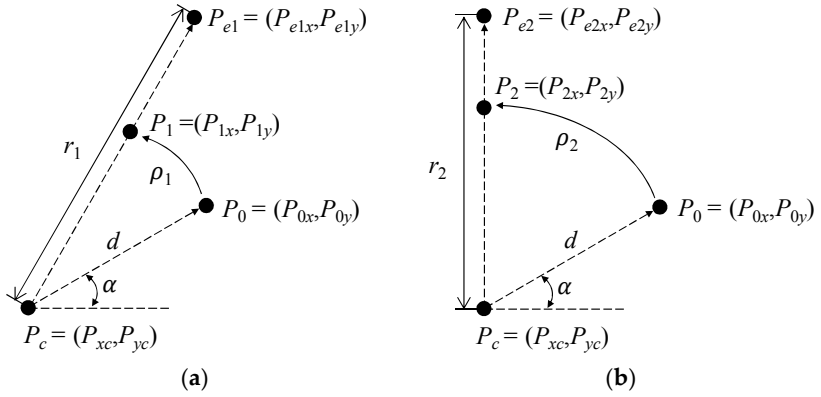

Figure 6. Schematic diagram of a point-cloud creation by an algorithmic approach. (**a**) First iteration; (**b**) Second iteration.

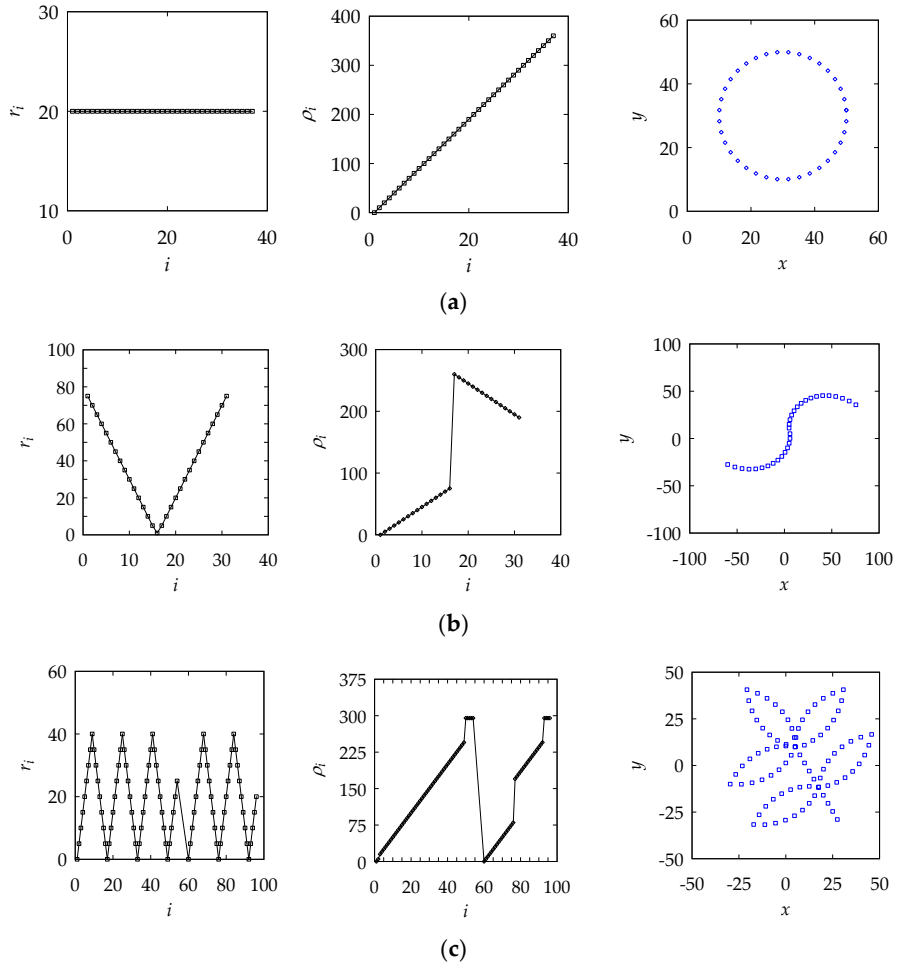

Figure 7. Point-cloud created by using the algorithmic approach. (**a**) Circle; (**b**) Curvy shape; (**c**) Leaf.

4. Cultural Heritage Preservation

RE based AM is used for digitizing, preserving, and restoring artifacts having cultural significance, as described in [27,60,61]. As far as the preservation of cultural heritage using RE technology is concerned, a great deal of work has been done based on the image processing technique. For example, Furferi et al. [62] have created a 2.5D model (tactical model) from paintings (i.e., 2D art) that is useful

for visually impaired and blind individuals to experience the content (historically significant paintings). The reconstruction process consists of mainly five steps, as follows: (1) Preliminary image processing for correcting the distortion and segmentation in the image; (2) Perspective geometric-based scene reconstruction for creating a 2.5D virtual object; (3) Volume reconstruction for retrieving the volumetric information of the 2.5D virtual object; (4) Virtual bas-relief reconstruction for integrating the outcomes of the steps 2 and 3; (5) Rapid prototyping of the virtual bas-relief. In this method, the explicit use of the point-cloud is not seen. In this study, the main focus is to employ the point-cloud for creating the artifacts which have cultural significance.

However, in RE based AM the point-clouds of the artifacts are obtained by using scanners, and processing the scanner created point-clouds for the sake of AM requires a great deal of computational efforts, as described in Section 2. Alternatively, one can use the method described in Section 3 to create the point-cloud without using a scanner. This section thus describes the application of the method described in Section 3 for digitizing, preserving, and restoring the cultural heritage relevant artifacts. In particular, the motifs relevant to Ainu culture is considered. The Ainu are indigenous peoples used to live in the northern part of the Japanese archipelago [63], namely, Hokkaido and Aomori. They also used to live in Sakhalin peninsula. The Ainu peoples often use exotic and unique motifs crafted on their clothing, houses, personal belongings, tools, and spiritual artifacts. Sometimes these motifs represent the identity of a segment of Ainu peoples living in a locality.

4.1. Classification of Ainu Motifs

Figure 8 shows some photographs of Ainu artifacts crafted with the motifs. The authors took the pictures at a souvenir shopping street located at the Akan Spa.

Figure 8. Some glimpses of Ainu motifs.

However, before creating the point-clouds of the motifs using the proposed method, it is important to study the types of the motifs. The Sapporo city authority provides a classification of Ainu motifs, as shown in Table 1 [64]. As seen in Table 1, the motif number 1 takes the shape of a thorn that is called Ayusi in Ainu language. The motif number 2 takes the shape of a spiral that is called Moreu

in Ainu language. The motif number 3 takes the shape of a spiral with small thorns that is called Arus-moreu in Ainu language. The motif number 4 takes the shape of a spiral with corners that is called Sikike-nu-moreu in Ainu language. The motif number 5 takes the shape of an eye that is called Sik in Ainu language. The motif number 6 takes the shape of intersects each other that is called Utasa in Ainu language. The motif number 7 takes the shape of two spirals that is called Uren-moreu in Ainu language. The motif number 8 takes the shape of two spirals shape with an eye that is called Ski-uren-moreu in Ainu language. The motif number 9 takes the shape of a spiral plant that is called Moreu-etok in Ainu language. The motif number 10 takes the shape of a vane that is called Punkar in Ainu language. The motif number 11 takes shape of a flower that is called Apapo-piras (u) ke in Ainu language. The motif number 12 takes shape of flower bud that is called Apapo-epuy in Ainu language. The motifs number 13 and 14 shapes do not have Ainu names, but they look like a heart type shape and a fishing bell shape, respectively. However, the motifs called Moreu, Sik, Utasa, and Ayusi are frequently used, and, thus, can be classified as the main motifs. The motifs called Arus-moreu, Sikike-nu-moreu, Sikike-nu-moreu, and Uren-moreu are created by modifying the main motifs, and, thus, can be classified as synthetic motifs. The motifs called Moreu-etok, Punkar, Apapo-piras (u) ke, and Apapo-epuy represent plants, and, thus, can be classified as the plant motifs. The other motifs (i.e., the motifs number 13 and number 14) can be classified as other motifs.

Table 1. Different types of Hokkaido-based Ainu motifs [64].

Number	Motif	Ainu Name	Description
1		Ayusi	A shape marked with thorn
2		Moreu	A spiral shape
3		Arus-moreu	A spiral shape with small thorns
4		Sikike-nu-moreu	A spiral shape with corners
5		Sik	An eye shape
6	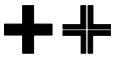	Utasa	A shape that intersects each other
7		Uren-moreu	Two spiral shapes
8		Ski-uren-moreu	Two spiral shapes with an eye shape
9		Moreu-etok	A shape like a spirally plant
10		Punkar	A shape like vine
11		Apapo-piras (u) ke	A shape like flower
12		Apapo-epuy	A shape like flower bud
13		-	A shape like heart type
14		-	A shape like fishing bell

4.2. Point-Cloud Creation

There are four main motifs as described above. The first three of them can be modeled by using the parametric-equation-based approach, whereas the other can be modeled by using the algorithmic approach.

First consider the point-clouds for representing the motifs called Moreu, Sik, and Utasa using the parametric-equation-based approach. The equation for representing the motif called Moreu is described as follows. Let $P_i = (P_{ix}, P_{iy})$ be an arbitrary point on the motif called Moreu. The equation of P_i is defined as follows.

$$P_{ix} = P_{0x} + a\theta_i \sin(\theta_i), P_{iy} = P_{0y} + b\theta_i \cos(\theta_i) \quad (1)$$

In Equation (1), $\theta_i = \theta_0 + (i-1)\Delta\theta$, $i = 1, ..., n$, $a, b > 0$, $b \geq a$, and $\Delta\theta > 0$. Figure 9a shows the point-cloud of Moreu in accordance with Equation (1), where $a = 0.15$, $b = 0.2$, $\theta_0 = 0°$, $\Delta\theta = 10°$, $n = 29$, $P_{0x} = 3$, and $P_{0y} = 3$.

Similarly, the equation for representing the motif called Sik is described as follows. Let $P_i = (P_{ix}, P_{iy})$ be an arbitrary point on the motif called Sik. The equation of P_i is defined as follows.

$$P_{ix} = P_{0x} + a\cos^3(\theta_i), P_{iy} = P_{0y} + b\sin^3(\theta_i), \quad (2)$$

In Equation (2), $\theta_i = \theta_0 + (i-1)\Delta\theta$, $i = 1, ..., n$, $a, b > 0$, $a = b$, $\Delta\theta > 0$, and $0 \leq \theta_i \leq 360$. Figure 9b shows the point-cloud of Sik in accordance with Equation (2), where $a = 2$, $b = 2$, $\theta_0 = 0°$, $\Delta\theta = 10°$, $n = 37$, $P_{0x} = 3$, and $P_{0y} = 3$. The third main motif called Utasa which takes shape of two lines intersected at mid-point. Thus, the point-cloud of Utasa can be created by using line Equation (A1) which is described in Section 3.1.

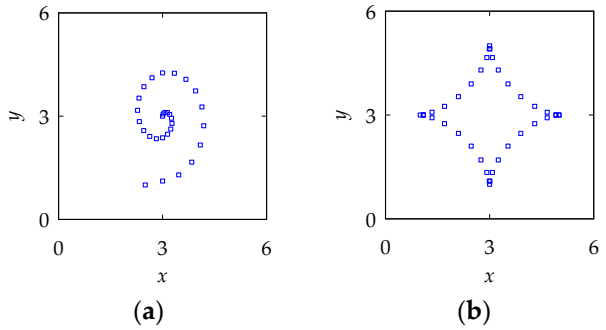

Figure 9. Point-clouds created using the parametric-equation-based approach. (**a**) Moreu; (**b**) Sik.

The fourth main motif called Ayusi cannot be created by using the parametric-equation-based approach. Thus, the Ayusi can be modeled using the algorithmic approach.

Figure 10 shows the point-cloud of Ayusi in accordance with the algorithm described in Section 3.2, for $\alpha = 0°$, $d = 10$, $P_{cx} = 0$, $P_{cy} = 2$, and where r_i and ρ_i are systematically adjusted for $i = 1, 2, \ldots, 85$. Some motifs can be created by combining both the parametric-equation-based approach and algorithmic approach, the example is shown in Figure 11. In Figure 11 the point-cloud of Series1 is created using the algorithmic approach and Series2 is created by using the parametric-equation-based approach.

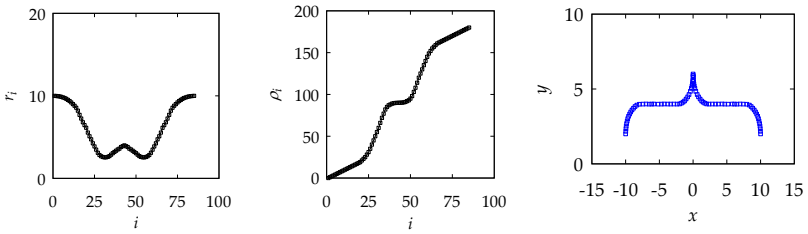

Figure 10. Point-clouds of Ayusi created using the algorithmic approach.

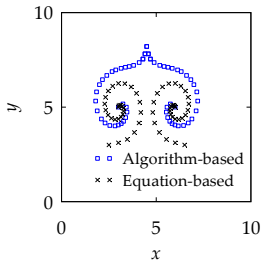

Figure 11. Point-clouds of Ski-uren-moreu created using both the algorithmic approach and parametric-equation-based approach.

4.3. CAD Modeling, Triangulation Modeling and AM

Based on the Ainu motifs, three models, namely, Model-1, Model-2, and Model-3 are created. This section describes the CAD Modeling, Triangulation Modeling, and execution of AM, as described in Figure 3, of Model-1, Model-2, and Model-3.

The Model-1 is created by using four Ski-uren-moreus and a Sik (shown in Figure 9b). Other three Ski-uren-moreus are obtained by rotation a Ski-uren-moreu as shown in Figure 11. The rotation is performed using Equations (A2) and (A3), where $\theta = \pi/2$, π, and $3\pi/2$. Combining all the point-clouds, the point-cloud of Model-1 is obtained as shown in Figure 12a. Now, the point-clouds of Model-1 is transferred to commercially available CAD package for CAD modeling. The result of the CAD modeling is shown in Figure 12b. Once the CAD modeling is done, the triangulation modeling is performed simply by saving the CAD model into an STL data file using a CAD package (the details are not shown to avoid commerciality). The result of triangulation modeling is shown in Figure 12c. The STL data generated from the triangulation modeling can be used to build a physical model of the Model-1 using AM devices (e.g., 3D printer) as shown in Figure 12d. In this case, an ordinary 3D printer is used (the details are not shown to avoid commerciality).

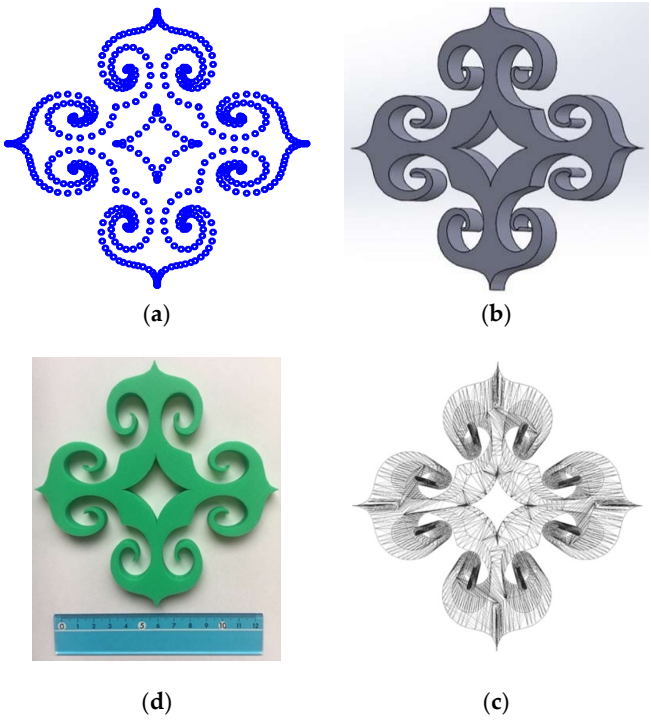

Figure 12. Model-1 based on Ainu motifs. (**a**) Point-cloud; (**b**) Solid CAD model; (**c**) Triangulation data; (**d**) Physical model built by 3D printer.

The Model-2 is created based on Moreu, Sik, and Utasa of main Ainu motifs. A total of twenty-four Moreus, eight Siks, one Utasa, and lines are used for creating the Model-2 as shown in Figure 13. The step-by-step point-clouds creation procedure of the Model-2 are as follows. Firstly, using Equation (A1), the point-cloud of Utasa and Square shape is created. Then, the point-clouds of two Moreu motifs are created so that they become symmetric about the y-axis. Next, the point-cloud of two lines are created to connect the point-clouds of the Moreu motifs to the point-cloud of a square. The same is done for the two other point-clouds of Moreu motifs, which are symmetrical about the y-axis. Then, point-cloud of Sik is created on top of the Moreu point-clouds. Now, the point-cloud of two connecting lines, Moreu, and Sik are rotated using Equations (A2) and (A3), where $\theta = \pi/2$, π, and $3\pi/2$. The same operation is repeated using Equations (A2) and (A3), where $\theta = \pi/4$, $3\pi/4$, $5\pi/4$, and $7\pi/4$, to complete the required point-cloud. The result is shown in Figure 13a. The CAD modeling, triangulation modeling, and AM process of Model-2 are performed similarly to the Model-1, as shown in Figure 13.

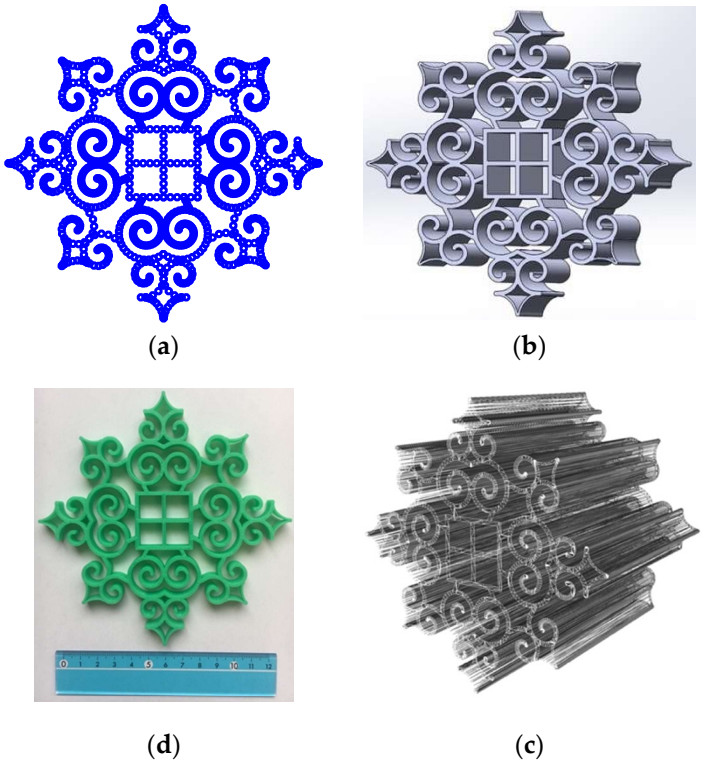

Figure 13. Model-2 based on Ainu motifs. (**a**) Point-cloud; (**b**) Solid CAD model; (**c**) Triangulation data; (**d**) Physical model built by 3D printing.

The Model-3 is created based on the Ainu motif shown in Figure 14a. It consists of Moreu, Sik, Ayusi, ellipses, curves, and lines. The point-cloud of Ayusi is created using the algorithmic approach and rest of the point-cloud are created using the parametric-equation-based approach which are in described in the previous section. Figure 14b shows the point-cloud of Ainu motif shown in Figure 14a. The CAD modeling, triangulation modeling, and AM process of Model-2 are performed similarly to the Model-1 and Model-2, as shown in Figure 14.

As seen from Figure 13, the Model-2 and Model-3 are more complicated than the Model-1, thus it consumes more time. It worth mentioning that while creating the point-cloud, it is better to start first from the center of a model and go outward. This step helps calculate the size of the shape and its location on the x-y plane. As shown in Figures 12 and 13, the models correspond to the main motifs (see Table 1). One can combine other motifs (e.g., synthetic, and plant motifs) to creates other

culturally significant artifacts of Ainus. Since the point-cloud creation process does not depend on the software package, it can be integrated with other devices used in the manufacturing of artifacts, e.g., 2D printing.

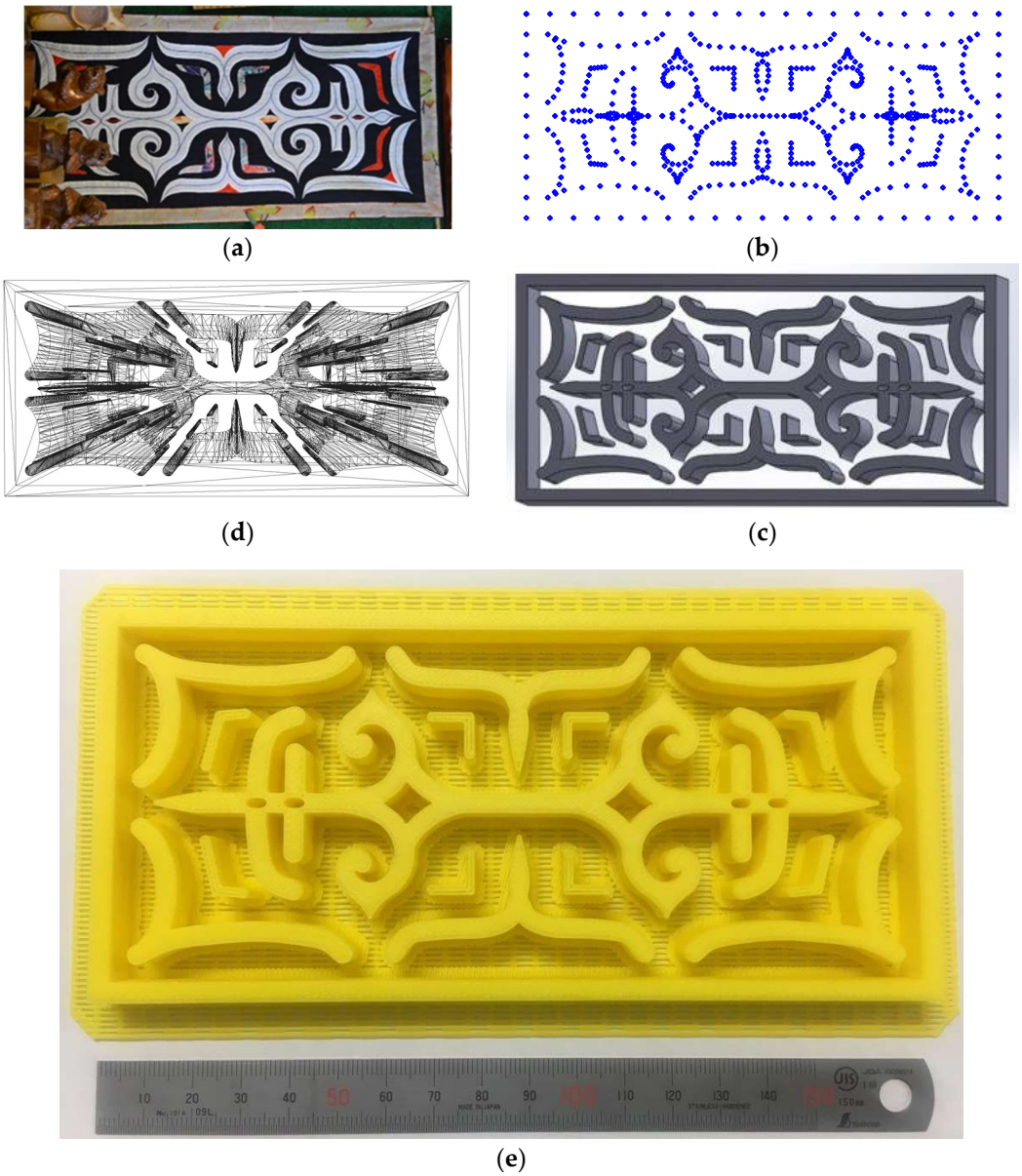

Figure 14. Model-3 based on Ainu motifs. (**a**) Ainu Motif; (**b**) Point-cloud; (**c**) Solid CAD Model; (**d**) Triangulation data; (**e**) Physical model built by 3D printing.

5. Concluding Remarks

Currently, the main emphasis of point-cloud based AM is on the point-clouds obtained by using a 3D scanner or by using image processing. An alternative approach can also equally be helpful, as demonstrated in the previous two sections. Particularly, the combination of the equation-based and algorithmic approach of creating point-clouds help create meaning objects, e.g., objects having cultural significance as shown in the previous section. In some cases, one can integrate the stochastic approach of creating point-cloud with the presented deterministic approach. This issue is open for further research. There are other open issues for future research, as well. For example, what if one superimposes the point-cloud obtained by a 3D scanner on the point-cloud obtained by the presented

approach? If the point-cloud obtained by the presented approach is considered the ideal point-cloud, then the point-cloud obtained by a 3D scanner can be processed based on the ideal one. This might open a new direction for PCAM. Nevertheless, as shown in the previous section, Ainu motifs can easily be modeled by the proposed PCAM, although the motifs are complex (i.e., having a complex structure of radius of curvature). As a result, one can use the proposed PCAM for creating aesthetic artifacts lucidly having complex geometry.

Author Contributions: Tashi, AMM Sharif Ullah, Michiko Watanabe, and Akihiko Kubo conceived the idea. Tashi and AMM Sharif Ullah conducted the literature review. Tashi, AMM Sharif Ullah and Michiko Watanabe developed the method. Tashi, AMM Sharif Ullah, and Akihiko Kubo developed the rapid prototypes. Tashi and AMM Sharif Ullah wrote the manuscript.

Conflicts of Interest: The authors declare no conflict of interest.

Appendix A. Details of Equation-Based Point-Clouds

Let $P_0 = (P_{0x}, P_{0y})$ and $P_1 = (P_{1x}, P_{1y})$ be the starting and end points of a straight-line in the x-y plane. Let $\forall t \in [0, 1]$ be the parameter. An arbitrary point, $P(t) = (P_x(t), P_y(t))$ between P_0 and P_1 is given as follows:

$$P_x(t) = P_{0x}(1-t) + P_{1x}(t) \qquad P_y(t) = P_{0y}(1-t) + P_{1y}(t) \tag{A1}$$

While creating a point-cloud using Equation (A1), the parameter is varied as follows: $t = 0, \Delta t, 2\Delta t, ..., 1$. Thus, the value of Δt decides the number of points in the point-cloud. In Figure 4, the point-cloud representing a straight-line is created using the abovementioned formulation.

A straight-line given by the point-cloud defined by Equation (A1) can be used as an edge of the face of a shape (e.g., a hexagon). In this case, one can rotate the point-cloud around the center of the shape to create other edges, as required. To be more specific, let $P_r = (P_{rx}, P_{ry})$ be the center of the shape and $P'(t) = (P'_x(t), P'_y(t))$ be the position of the point, $P(t) = (P_x(t), P_y(t))$ after its rotation around $P_r = (P_{rx}, P_{ry})$ in the counter-clockwise direction by an angle θ. Thus, the following formulation holds:

$$P'_x(t) = P_{rx} + (P_x(t) - P_{rx})\cos\theta - \left(P_y(t) - P_{ry}\right)\sin\theta \tag{A2}$$

$$P'_y(t) = P_{ry} + (P_x(t) - P_{rx})\sin\theta + \left(P_y(t) - P_{ry}\right)\cos\theta \tag{A3}$$

The formulation defined by Equations (A2) and (A3) is used five times to create the five point-clouds of the five edges from the point-cloud of the first edge for $\theta = \pi/3, 2\pi/3, \pi, 4\pi/3$, and $5\pi/3$. This way one can create the face of any shape in terms of point-clouds.

Let $P_c = (P_{cx}, P_{cy})$ be a center of ellipse in the x-y plane. Let $\forall t \in [0, 1]$ be the parameter. Consider, a and b are major and minor radius of the ellipse, respectively. For ellipse, $a, b > 0$ and $a > b$. An arbitrary point, $P(t) = (P_x(t), P_y(t))$ is given by

$$P_x(t) = P_{cx} + a\cos(2\pi t)\ P_y(t) = P_{cy} + b\cos(2\pi t) \tag{A4}$$

While creating a point-cloud using Equation (A4), the parameter is varied as follows: $t = -1, -1 + \Delta t, -1 + 2\Delta t, ..., 1$. Thus, the value of Δt decides the number of points in the point-cloud. In Figure 4, the point-cloud representing the ellipse is created using the abovementioned formulation.

Let $P(t) = (P_x(t), P_y(t))$ be an arbitrary point in the x-y plane. Let $\forall t \in [-1, 1]$ be the parameter. A curve called Bicorn curve is given as follows:

$$P_x(t) = \sin(\pi t) \qquad P_y(t) = \frac{\cos^2(\pi t)(2 + \cos(\pi t))}{3 + \sin^2(\pi t)} \tag{A5}$$

While creating a point-cloud using Equation (A5), the parameter is varied as follows: $t = -1$, $-1 + \Delta t$, $-1 + 2\Delta t$, ..., 1. Thus, the value of Δt decides the number of points in the point-cloud. In Figure 4, the point-cloud representing the Bicorn curve is created using the abovementioned formulation.

References

1. Gibson, I.; Rosen, D.; Stucker, B. *Additive Manufacturing Technologies: 3D Printing, Rapid Prototyping, and Direct Digital Manufacturing*, 2nd ed.; Springer: New York, NY, USA, 2015.
2. Thompson, M.K.; Moroni, G.; Vaneker, T.; Fadel, G.; Campbell, R.I.; Gibson, I.; Bernard, A.; Schulz, J.; Graf, P.; Ahuja, B.; et al. Design for Additive Manufacturing: Trends, opportunities, considerations, and constraints. *CIRP Ann.* **2016**, *65*, 737–760. [CrossRef]
3. Gao, W.; Zhang, Y.; Ramanujan, D.; Ramani, K.; Chen, Y.; Williams, C.B.; Wang, C.C.; Shin, Y.C.; Zhang, S.; Zavattieri, P.D. The status, challenges, and future of additive manufacturing in engineering. *Comput.-Aided Des.* **2015**, *69*, 65–89. [CrossRef]
4. Bourell, D.L.; Rosen, D.W.; Leu, M.C. The Roadmap for Additive Manufacturing and Its Impact. *3D Print. Addit. Manuf.* **2014**, *1*, 6–9. [CrossRef]
5. Hirz, M.; Rossbacher, P.; Gulanová, J. Future trends in CAD—From the perspective of automotive industry. *Comput.-Aided Des. Appl.* **2017**, *14*, 734–741. [CrossRef]
6. Yap, Y.L.; Tan, Y.S.; Tan, H.K.; Peh, Z.K.; Low, X.Y.; Yeong, W.Y.; Tan, C.S.; Laude, A. 3D printed bio-models for medical applications. *Rapid Prototyp. J.* **2017**, *23*, 227–235. [CrossRef]
7. Hieu, L.C.; Zlatov, N.; Vander Sloten, J.; Bohez, E.; Khanh, L.; Binh, P.H.; Oris, P.; Toshev, Y. Medical rapid prototyping applications and methods. *Assem. Autom.* **2005**, *25*, 284–292. [CrossRef]
8. Sun, W.; Starly, B.; Nam, J.; Darling, A. Bio-CAD modeling and its applications in computer-aided tissue engineering. *Comput.-Aided Des.* **2005**, *37*, 1097–1114. [CrossRef]
9. Mannoor, M.S.; Jiang, Z.; James, T.; Kong, Y.L.; Malatesta, K.A.; Soboyejo, W.O.; Verma, N.; Gracias, D.H.; McAlpine, M.C. 3D Printed Bionic Ears. *Nano Lett.* **2013**, *13*, 2634–2639. [CrossRef] [PubMed]
10. Steffan, D.; Dominic, E. A CAD and AM process for maxillofacial prostheses bar-clip retention. *Rapid Prototyp. J.* **2016**, *22*, 170–177. [CrossRef]
11. Luximon, Y.; Ball, R.M.; Chow, E.H.C. A design and evaluation tool using 3D head templates. *Comput.-Aided Des. Appl.* **2016**, *13*, 153–161. [CrossRef]
12. Jung, W.; Park, S.; Shin, H. Combining volumetric dental CT and optical scan data for teeth modeling. *Comput.-Aided Des.* **2015**, *67–68*, 24–37. [CrossRef]
13. Urbanic, R.J. From thought to thing: Using the fused deposition modeling and 3D printing processes for undergraduate design projects. *Comput.-Aided Des. Appl.* **2016**, *13*, 768–785. [CrossRef]
14. Galina, L.; Na, X. Academic library innovation through 3D printing services. *Libr. Manag.* **2017**, *38*, 208–218. [CrossRef]
15. Heather, M.M.-L. Makers in the library: Case studies of 3D printers and maker spaces in library settings. *Libr. Hi Tech* **2014**, *32*, 583–593. [CrossRef]
16. Wannarumon, S.; Bohez, E.L.J. A New Aesthetic Evolutionary Approach for Jewelry Design. *Comput.-Aided Des. Appl.* **2006**, *3*, 385–394. [CrossRef]
17. 3DR Holdings, LLC. 3D Printed Clothing. October 2017. Available online: https://3dprint.com/tag/3d-printed-clothing/ (accessed on 15 November 2017).
18. Balance, N. The Future of Running Is Here. April 2016. Available online: https://www.newbalance.com/article?id=4041 (accessed on 16 November 2017).
19. i.materialize. 3D Printed Fashion: 10 Amazing 3D Printed Dresses. 2017. Available online: https://i.materialise.com/blog/3d-printed-fashion-dresses/ (accessed on 15 November 2017).
20. Nike. Nike Debuts First-Ever Football Cleat Built Using 3D Printing Technology. February 2013. Available online: https://news.nike.com/news/nike-debuts-first-ever-football-cleat-built-using-3d-printing-technology (accessed on 16 November 2017).
21. Sun, J.; Zhou, W.; Yan, L.; Huang, D.; Lin, L.Y. Extrusion-based food printing for digitalized food design and nutrition control. *J. Food Eng.* **2018**, *220* (Suppl. C), 1–11. [CrossRef]
22. Lin, C. 3D Food Printing: A Taste of the Future. *J. Food Sci. Educ.* **2015**, *14*, 86–87. [CrossRef]
23. Ferreira, I.A.; Alves, J.L. Low-cost 3D food printing. *Ciênc. Tecnol. Mater.* **2017**, *29*, e265–e269. [CrossRef]

24. Sakin, M.; Kiroglu, Y.C. 3D Printing of Buildings: Construction of the Sustainable Houses of the Future by BIM. *Energy Procedia* **2017**, *134* (Suppl. C), 702–711. [CrossRef]
25. Hager, I.; Golonka, A.; Putanowicz, R. 3D Printing of Buildings and Building Components as the Future of Sustainable Construction? *Procedia Eng.* **2016**, *151* (Suppl. C), 292–299. [CrossRef]
26. Lim, S.; Buswell, R.A.; Le, T.T.; Austin, S.A.; Gibb, A.G.; Thorpe, T. Developments in construction-scale additive manufacturing processes. *Autom. Constr.* **2012**, *21* (Suppl. C), 262–268. [CrossRef]
27. Scopigno, R.; Cignoni, P.; Pietroni, N.; Callieri, M.; Dellepiane, M. Digital Fabrication Techniques for Cultural Heritage: A Survey. In *Computer Graphics Forum*; Wiley: Hoboken, NJ, USA, 2017; Volume 36, pp. 6–21. [CrossRef]
28. Conner, B.P.; Manogharan, G.P.; Meyers, K.L. An assessment of implementation of entry-level 3D printers from the perspective of small businesses. *Rapid Prototyp. J.* **2015**, *21*, 582–597. [CrossRef]
29. Holzmann, P.; Breitenecker, R.J.; Soomro, A.A.; Schwarz, E.J. User entrepreneur business models in 3D printing. *J. Manuf. Technol. Manag.* **2017**, *28*, 75–94. [CrossRef]
30. Camille, B. What are you printing? Ambivalent emancipation by 3D printing. *Rapid Prototyp. J.* **2015**, *21*, 572–581. [CrossRef]
31. James, D.W.; Belblidia, F.; Eckermann, J.E.; Sienz, J. An innovative photogrammetry color segmentation based technique as an alternative approach to 3D scanning for reverse engineering design. *Comput.-Aided Des. Appl.* **2017**, *14*, 1–16. [CrossRef]
32. Masuda, H.; Niwa, T.; Tanaka, I.; Matsuoka, R. Reconstruction of Polygonal Faces from Large-Scale Point-Clouds of Engineering Plants. *Comput.-Aided Des. Appl.* **2015**, *12*, 555–563. [CrossRef]
33. Krznar, N.; Pilipović, A.; Šercer, M. Additive Manufacturing of Fixture for Automated 3D Scanning—Case Study. *Procedia Eng.* **2016**, *149* (Suppl. C), 197–202. [CrossRef]
34. Várady, T.; Martin, R.R.; Cox, J. Reverse engineering of geometric models—An introduction. *Comput.-Aided Des.* **1997**, *29*, 255–268. [CrossRef]
35. Paulic, M.; Irgolic, T.; Balic, J.; Cus, F.; Cupar, A.; Brajlih, T.; Drstvensek, I. Reverse Engineering of Parts with Optical Scanning and Additive Manufacturing. *Procedia Eng.* **2014**, *69* (Suppl. C), 795–803. [CrossRef]
36. Nooran, R. *3D Printing: Technology, Applications, and Selection*, 1st ed.; CRC Press: Boca Raton, FL, USA, 2018.
37. Yang, J.; Cao, Z.; Zhang, Q. A fast and robust local descriptor for 3D point cloud registration. *Inf. Sci.* **2016**, *346–347* (Suppl. C), 163–179. [CrossRef]
38. Li, W.; Song, P. A modified ICP algorithm based on dynamic adjustment factor for registration of point cloud and CAD model. *Pattern Recognit. Lett.* **2015**, *65* (Suppl. C), 88–94. [CrossRef]
39. Zhao, X.; Ilieş, H.T. Learned 3D shape descriptors for classifying 3D point cloud models. *Comput.-Aided Des. Appl.* **2017**, *14*, 507–515. [CrossRef]
40. Watanabe, T.; Niwa, T.; Masuda, H. Registration of Point-Clouds from Terrestrial and Portable Laser Scanners (Special Issue on Digital Engineering for Complex Shapes). *Int. J. Autom. Technol.* **2016**, *10*, 163–171. [CrossRef]
41. Syed, H.M.; Mohammed, A.M.; Abdulrahman, M.A.-A. The influence of surface topology on the quality of the point cloud data acquired with laser line scanning probe. *Sens. Rev.* **2014**, *34*, 255–265. [CrossRef]
42. Lee, K.H.; Woo, H. Direct integration of reverse engineering and rapid prototyping. *Comput. Ind. Eng.* **2000**, *38*, 21–38. [CrossRef]
43. Fayolle, P.-A.; Pasko, A. An evolutionary approach to the extraction of object construction trees from 3D point clouds. *Comput.-Aided Des.* **2016**, *74* (Suppl. C), 1–17. [CrossRef]
44. Schwartz, A.; Schneor, R.; Molcho, G.; Weiss Cohen, M. Surface detection and modeling of an arbitrary point cloud from 3D sketching. *Comput.-Aided Des. Appl.* **2017**, 1–11. [CrossRef]
45. Xu, J.; Hou, W.; Zhang, H. An improved virtual edge approach to slicing of point cloud for additive manufacturing. *Comput.-Aided Des. Appl.* **2017**, 1–7. [CrossRef]
46. Huang, H.; Mok, P.Y.; Kwok, Y.L.; Au, J.S. Automatic Block Pattern Generation from a 3D Unstructured Point Cloud. *Res. J. Text. Appar.* **2010**, *14*, 26–37. [CrossRef]
47. Peternell, M.; Steiner, T. Reconstruction of piecewise planar objects from point clouds. *Comput.-Aided Des.* **2004**, *36*, 333–342. [CrossRef]
48. Pralay, P. An easy rapid prototyping technique with point cloud data. *Rapid Prototyp. J.* **2001**, *7*, 82–90. [CrossRef]

49. Oropallo, W.; Piegl, L.A.; Rosen, P.; Rajab, K. Generating point clouds for slicing free-form objects for 3-D printing. *Comput.-Aided Des. Appl.* **2017**, *14*, 242–249. [CrossRef]
50. Oropallo, W.; Piegl, L.A.; Rosen, P.; Rajab, K. Point cloud slicing for 3-D printing. *Comput.-Aided Des. Appl.* **2018**, *15*, 90–97. [CrossRef]
51. Ma, J.; Chen, J.S.; Feng, H.Y.; Wang, L. Automatic construction of watertight manifold triangle meshes from scanned point clouds using matched umbrella facets. *Comput.-Aided Des. Appl.* **2017**, *14*, 742–750. [CrossRef]
52. Zhong, S.; Yang, Y.; Huang, Y. Data Slicing Processing Method for RE/RP System Based on Spatial Point Cloud Data. *Comput.-Aided Des. Appl.* **2014**, *11*, 20–31. [CrossRef]
53. Yang, P.; Schmidt, T.; Qian, X. Direct Digital Design and Manufacturing from Massive Point-Cloud Data. *Comput.-Aided Des. Appl.* **2009**, *6*, 685–699. [CrossRef]
54. Percoco, G.; Galantucci, L.M. Local-genetic slicing of point clouds for rapid prototyping. *Rapid Prototyp. J.* **2008**, *14*, 161–166. [CrossRef]
55. Chang, M.-C.; Leymarie, F.F.; Kimia, B.B. Surface reconstruction from point clouds by transforming the medial scaffold. *Comput. Vis. Image Underst.* **2009**, *113*, 1130–1146. [CrossRef]
56. Sharif Ullah, A.M.M.; Sato, Y.; Kubo, A.; Tamaki, J.I. Design for Manufacturing of IFS Fractals from the Perspective of Barnsley's Fern-leaf. *Comput.-Aided Des. Appl.* **2015**, *12*, 241–255. [CrossRef]
57. Ullah, A.M.M.S.; D'Addona, D.M.; Harib, K.H.; Lin, T. Fractals and Additive Manufacturing. *Int. J. Autom. Technol.* **2016**, *10*, 222–230. [CrossRef]
58. Ullah, A.M.M.S.; Omori, R.; Nagara, Y.; Kubo, A.; Tamaki, J. Toward Error-free Manufacturing of Fractals. *Procedia CIRP* **2013**, *12* (Suppl. C), 43–48. [CrossRef]
59. Sharif Ullah, A.M.M. Design for additive manufacturing of porous structures using stochastic point-cloud: A pragmatic approach. *Comput.-Aided Des. Appl.* **2018**, *15*, 138–146. [CrossRef]
60. Neumüller, M.; Reichinger, A.; Rist, F.; Kern, C. 3D Printing for Cultural Heritage: Preservation, Accessibility, Research and Education. In *3D Research Challenges in Cultural Heritage*; Ioannides, M., Quak, E., Eds.; Lecture Notes in Computer Science; Springer: Berlin/Heidelberg, Germany, 2014; Volume 8355, pp. 119–134.
61. Hess, M.; Robson, S. Re-engineering Watt: A case study and best practice recommendations for 3D colour laser scans and 3D printing in museum artefact documentation. In *Lacona IX—Lasers in Conservation*; Archetype Publications: London, UK, 2013; pp. 154–162.
62. Furferi, R.; Governi, L.; Volpe, Y.; Puggelli, L.; Vanni, N.; Carfagni, M. From 2D to 2.5D i.e. from painting to tactile model. *Graph. Models* **2014**, *76*, 706–723. [CrossRef]
63. Cheung, S.C.H. Ainu culture in transition. *Futures* **2003**, *35*, 951–959. [CrossRef]
64. Introduction of Traditional Crafts: Ainushiriki. 2016. Available online: http://www.city.sapporo.jp/shimin/pirka-kotan/jp/kogei/ainu-siriki/ (accessed on 15 January 2018).